Comparison of the expression and toxicity of AAV2/9 carrying the human A53T α-synuclein gene in presence or absence of WPRE

Xiuping Sun, Xuan Yu, Ling Zhang, Wenjie Zhao, Manshi Wang, Yu Zhang, Xianglei Li, Ran Gao, Ludivine Breger, Sandra Dovero, et al.

▶ **To cite this version:**

Xiuping Sun, Xuan Yu, Ling Zhang, Wenjie Zhao, Manshi Wang, et al.. Comparison of the expression and toxicity of AAV2/9 carrying the human A53T α-synuclein gene in presence or absence of WPRE. Heliyon, 2021, 7 (2), pp.e06302. 10.1016/j.heliyon.2021.e06302 . inserm-03154753

HAL Id: inserm-03154753

https://inserm.hal.science/inserm-03154753

Submitted on 1 Mar 2021

HAL is a multi-disciplinary open access archive for the deposit and dissemination of scientific research documents, whether they are published or not. The documents may come from teaching and research institutions in France or abroad, or from public or private research centers.

L'archive ouverte pluridisciplinaire **HAL**, est destinée au dépôt et à la diffusion de documents scientifiques de niveau recherche, publiés ou non, émanant des établissements d'enseignement et de recherche français ou étrangers, des laboratoires publics ou privés.

Heliyon 7 (2021) e06302

Contents lists available at ScienceDirect

Heliyon

journal homepage: www.cell.com/heliyon

Research article

Comparison of the expression and toxicity of AAV2/9 carrying the human A53T α-synuclein gene in presence or absence of WPRE

Xiuping Sun [a], Xuan Yu [a], Ling Zhang [a], Wenjie Zhao [a], Manshi Wang [a], Yu Zhang [a], Xianglei Li [a], Ran Gao [a], Ludivine S. Breger [b], Sandra Dovero [b], Gregory Porras [b], Pierre-Olivier Fernagut [b,c], Benjamin Dehay [b], Erwan Bezard [a,b,*], Chuan Qin [a,**]

[a] NHC Key Laboratory of Human Disease Comparative Medicine, Beijing Engineering Research Center for Experimental Animal Models of Human Critical Diseases, Peking Union Medical College (PUMC) & Institute of Laboratory Animal Science, Chinese Academy of Medical Science (CAMS), Beijing, China
[b] Univ. Bordeaux, CNRS, IMN, UMR 5293, F-33000 Bordeaux, France
[c] Université de Poitiers, Laboratoire de Neurosciences Expérimentales et Cliniques, INSERM UMR_S 1084, Poitiers, France

ARTICLE INFO

Keywords:
Parkinson's disease
Synucleinopathy
Woodchuck hepatitis virus post-transcriptional regulatory element
Mouse

ABSTRACT

Woodchuck Hepatitis Virus Post-transcriptional Regulatory Element (WPRE) is thought to enhance transgene expression of target genes delivered by adeno-associated viral (AAV) vectors. This study assessed the protein expression of α-synuclein, phosphorylated α-synuclein at Serine 129, extent of nigrostriatal degeneration as well as subsequent behavioral deficits induced by unilateral intranigral stereotactic injection in male adult C57BL/6J mice of an AAV2/9 expressing A53T human α-synuclein under the control of the synapsin promoter in presence or absence of the WPRE. The presence of WPRE enabled to achieve greater nigrostriatal degeneration and synucleinopathy which was concomitant with worsened forelimb use asymmetry. This work refines a mouse Parkinson's disease model in which anatomo-pathology is related to behavioral deficits.

1. Introduction

Parkinson's disease (PD) is a slowly progressive neurodegenerative disorder marked by the selective loss of dopaminergic neurons in the substantia nigra pars compacta (SNpc) and the presence of proteinaceous inclusions named Lewy bodies (LB) in surviving neurons and Lewy neurites in cell processes (Kalia and Lang, 2015). α-synuclein (α-syn) is a major constituent of LB and the first disease-causing protein characterized in both sporadic and familial PD (Dehay et al., 2015). Several α-syn-based animal models of PD have been developed to investigate the pathophysiology of PD, notably through viral vector-mediated overexpression of the wild-type (WT) or mutated *SNCA* gene. Lentiviral (LV) or adeno-associated (AAV) viral vector-mediated overexpression of *SNCA* gene has been successfully conducted in several species, including mice, rats and non-human primates (Bourdenx et al., 2015; Kirik et al., 2003; Koprich et al., 2010; Lo Bianco et al., 2002; Oliveras-Salvá et al., 2013). Surprisingly, the largest extent of lesion is observed in rats compared to mice and non-human primates, with subsequent overt motor and non-motor symptoms in the AAV-α-synuclein rat (Engeln et al., 2016) (Engeln et al., 2013) but not in mice or non-human primates (Bourdenx et al., 2015; Koprich et al., 2016). Beyond possible, but yet to be fully investigated, inter-species and intra-species differences (Bourdenx et al., 2015) the vector type, the serotype for AAVs or the titers are obvious variables (McFarland et al., 2009; St Martin et al., 2007). The introduction of additional elements such as woodchuck hepatitis virus post-transcriptional regulatory element (WPRE), described for enhancing transgene expression (Hollensen et al., 2017; Klein et al., 2006; Zufferey et al., 1999), often lacks head to head comparison for ascertaining the toxicity enhancement it is supposed to afford but in a minority of papers such as (Decressac et al., 2012). We previously reported that AAV2/9-mediated mutated human A53T α-syn overexpression induces nigrostriatal neurodegeneration in mice, rats and non-human primates (Arotcarena et al., 2019; Bido et al., 2017; Novello et al., 2018) while displaying considerable lesser efficiency in the mouse than in other species (Bourdenx et al., 2015). We here investigate in a proper head-to-head comparison whether WPRE can enhance the overexpression of AAV2/9 mediated A53T human α-synuclein in the

* Corresponding author.
** Corresponding author.
E-mail addresses: erwan.bezard@u-bordeaux.fr (E. Bezard), chuanqin@vip.sina.com (C. Qin).

https://doi.org/10.1016/j.heliyon.2021.e06302
Received 10 September 2020; Received in revised form 25 November 2020; Accepted 12 February 2021
2405-8440/© 2021 The Author(s). Published by Elsevier Ltd. This is an open access article under the CC BY-NC-ND license (http://creativecommons.org/licenses/by-nc-nd/4.0/).

C57BL/6J mice, for generating a PD-relevant extent of lesion and pathology.

2. Material and methods

2.1. Animals

20 male wild type C57BL/6J mice aged 6 weeks were purchased from Beijing HFK Bioscience Co. and habituated to the animal facility for two weeks prior starting the experiments. All the animals were kept under standard housing conditions (22–25 °C with a 12 h/12 h light/dark cycle) and received standard food and tap water *ad libitum*. The study was approved by the ethical committee for the use of experimental animals of the Institute of Laboratory Animal Sciences (license number: 17002).

2.2. AAV vector production

AAV2/9-synapsin-synA53T (i.e.A53T) and AAV2/9-synapsin-synA53T-WPRE (i.e.A53T-WPRE) vectors were produced by polyethylenimine (PEI) mediated triple transfection of low passage HEK-293 T/17 cells (ATCC; cat number CRL-11268). The respective AAV expression plasmids were cotransfected with the adeno helper pAd Delta F6 plasmid (Penn Vector Core, cat # PL-F-PVADF6) and AAV Rep Cap pAAV2/9 plasmid (Penn Vector Core, cat # PL-TPV008). AAV vectors were purified as previously described (Bourdenx et al., 2015). Cells are harvested 72 h post transfection, resuspended in lysis buffer (150 mM NaCl, 50 mM Tris–HCl pH 8.5) and lysed by 3 freeze-thaw cycles (37 °C/-80 °C). The cell lysate is treated with 150 units/ml Benzonase (Sigma, St Louis, MO) for 1 h at 37 °C and the crude lysate is clarified by centrifugation. Vectors are purified by iodixanol step gradient centrifugation, and concentrated and buffer-exchanged into Lactated Ringer's solution (Baxter, Deerfield, IL) using vivaspin20 100 kDa cut off concentrator (Sartorius Stedim, Goettingen, Germany). Titrations were performed at the transcriptome core facility (Neurocentre Magendie, INSERM U862, Bordeaux, France). The genome-containing particle (gcp) titer was determined at a concentration of 5.16×10^{12}

gcp/ml by quantitative real-time PCR using the Light Cycler 480 SYBR green master mix (Roche, cat # 04887352001) with primers specific for the AAV2 ITRs (fwd 5′-GGAACCCCTAGTGATG GAGTT-3'; rev 5′-CGGCCTCAGTGAGCGA-3′) on a Light Cycler 480 instrument. Purity assessment of vector stocks was estimated by loading 10 μl of vector stock on 10 % SDS acrylamide gels, total proteins were visualized using the Krypton Infrared Protein Stain according to the manufacturer's instructions (Life Technologies).

2.3. Surgical procedures

All the interventions were performed under full general anaesthesia with isoflurane in oxygen-enriched air (12 %). Mice were placed in a stereotaxic frame (Kopf Instruments) and received one unilateral intranigral injection (AP -2.9 mm; ML-1.3 mm; DV -4.5 mm from Bregma) of either 1 μl of AAV2/9-synapsin-synA53T or 1 μl AAV2/9-synapsin-synA53T-WPRE (concentration:1.02×10^{13} gcp/ml) at a rate of 0.4 μl/min as previously described (Bourdenx et al., 2015). The pipette was left in place for 5 min after injection to avoid leakage. After surgery, mice were placed in an incubator for optimized recovery from anaesthesia.

2.4. Behavioral tests

Cylinder test and challenging beam test were conducted 12 weeks after AAV2/9 injection. The videos of the behavioral tests were viewed and scored in slow motion by an observer blind to the treatment condition. To assess forelimb asymmetry, mice were placed into a transparent plexiglass cylinder (diameter: 9.5 cm, height: 20 cm) and videotaped for 3 min. Contacts made with the ipsilateral (right) forelimb, contralateral (left) forelimb or both forelimbs and the wall of the plexiglas cylinder were counted by an experimenter blind to the experimental condition. The percentage of ipsilateral and contralateral contacts, relative to the total number of contacts, was calculated. An asymmetry index was calculated as: (Ipsilateral forelimb − Contralateral forelimb)/(Ipsilateral forelimb + Contralateral forelimb + Both movement).

Motor coordination was assessed using the challenging beam test as previously described (Fleming et al., 2013; Soria et al., 2017). Mice were first trained for 5 trials per day on three consecutive days to traverse a beam composed of four sections (25 cm each) of decreasing width (3.5 cm–0.5 cm) and leading to the animal's home cage. On the fourth day, a mesh grid (1 cm^2) that corresponds to each beam width was placed on top of each beam section. Testing was performed on the next day and the five trials were videotaped for each mouse. Videos were rated blindly for the number of errors, number of steps, and time to traverse the beam. Errors per step was calculated as the number of errors divided by the number of steps.

2.5. Immunohistochemistry

Immediately after completion of the behavioral tests, i.e. at 12 weeks post-surgery, mice were anesthetized with sodium pentobarbital (100 mg/kg body weight, i.p.) and perfused with 0.9% NaCl followed by ice cold 4% paraformaldehyde (PFA). Brains were post-fixed for 24 h in 4% PFA, then cryoprotected in 20% sucrose in 0.1M PBS. Brains were frozen in isopentane and stored at -80 °C. 50 μm free-floating coronal sections of the entire striatum and midbrain were collected for histological analysis. Immunohistochemistry was performed for each animal on striatum (from 1 to 3 sections) and on every fourth midbrain sections spanning the entire rostro-caudal SNpc. Selected sections were incubated all together overnight with primary antibodies for the following antigens: TH (1:5.000 clone EP1532Y, ab137869 Abcam), α-synuclein (1:1.000 clone Syn211, Thermo Scientific, MS1572), or phosphorylated Ser129 α-synuclein (1:5.000, EP1536Y, ab51253, Abcam). Immunoreactions were revealed by an anti–species dependent peroxidase EnVisionTM system (DAKO) followed by DAB visualization. Sections were mounted on gelatinized slides, counterstained with 0.1% cresyl violet solution if needed, dehydrated, and cover-slipped.

2.6. Image analysis

TH-positive SNpc cells were counted by stereology, using a Leica DM-6000B microscope coupled with the Mercator Pro software (Explora Nova). The SNpc was delineated for each section, and probes for stereological counting were applied to the map obtained (probe size was 50 × 40 spaced by 150 × 120μm). Only TH-positive cells with its nucleus included in the probe or crossing the green line of the probe were counted. The total number of TH-positive cells within the whole nigra was estimated using the optical fractionator method.

The TH staining in the striatum was quantified by optical density (OD). Sections were scanned with an Epson expression 10000XL high-resolution scanner. Images were first opened in ImageJ open-source software (ImageJ.nih.gov). Brightness and contrast were set to optimize the histogram of images. The same parameters were applied for all images of the same staining in order to compare the mean grey value for each striatum without any bias.

For the α-synuclein and phosphorylated α-synuclein staining, high-resolution whole color slide images were first acquired with the 3DHistech Panoramic Scanner at 20 × magnification, with 5 layers in extended mode. Each image was opened in the off-line Mercator Pro software (Explora Nova), and the mapping of all regions of interest was made. Then the threshold surface analysis was conducted to quantify antibody-based staining in the region of interest as previously described (Arotcarena et al., 2019). Briefly, brightness and contrast rules were applied to the RGB pictures to optimize details without any saturation of the image. The color thresholding tool was then used to select the threshold corresponding to the brown color revealed by the DAB staining. The threshold

has been established on the basis of the staining intensity to detect the maximum of DAB staining. In each region, the software extracted the surface corresponding to the threshold defined. The surface parameter was finally expressed as a ratio of the total surface of each area of interest.

2.7. Statistical analysis

All results are presented as mean ± standard error of the mean (SEM) and were compared by two-way ANOVA with AAV type and hemisphere/hemibody as independent variables, followed by Tukey's multiple comparison tests (GraphPad Prism 9).

3. Results

3.1. Both vectors achieved α-syn overexpression

Both AAV2/9-synapsin-synA53T and AAV2/9-synapsin-synA53T-WPRE resulted in a widespread protein expression of α-syn in the ipsilateral side (injection) of SNpc (Figure 1). AAV-mediated overexpression of α-syn led to diffusion of α-syn throughout the ipsilateral side mostly at the level of the mesencephalon with lesser diffusion to the contralateral (non-injected) side (Figure 1 D-F). In the SNpc, there was an AAV construct × hemisphere interaction ($F_{(1,36)} = 9.950$, $P = 0.003$), an effect of AAV construct ($F_{(1, 36)} = 23.42$, $p < 0.0001$) and of hemisphere ($F_{(1, 36)} = 3699$, $P < 0.0001$). Post-hoc analysis showed however no difference in α-syn expression level in SNpc between the AAV2/9-synapsin-synA53T and AAV2/9-synapsin-synA53T-WPRE mice ($p = 0.6359$).

Extensive human specific α-syn staining was detected throughout the ipsilateral striatum, indicating either a retrograde AAV uptake or the transport of the α-syn protein itself from the SNpc neurons to their terminals in the striatum (Figure 1 A-C). At the striatal level (Figure 1 A-C), diffusion was not observed massively in the contralateral side but a clear presence of few fibers positive for α-syn can be observed in the contralateral striatum (insets in Figure 1 A-B). In the striatum, there was no AAV construct × hemisphere interaction ($F_{(1,36)} = 0.9956$, $P = 0.3250$), no effect of AAV construct ($F_{(1, 36)} = 1.134$, $p = 0.2941$) but an effect of hemisphere ($F_{(1, 36)} = 785.4$, $P < 0.0001$). Post-hoc analysis showed however no difference in α-syn expression level in striatum between the AAV2/9-synapsin-synA53T and AAV2/9-synapsin-synA53T-WPRE mice ($p = 0.4725$).

3.2. AAV2/9-synapsin-synA53T -WPRE displayed greater nigrostriatal degeneration

In the SNpc, the two way ANOVA revealed no AAV construct × hemisphere interaction ($F_{(1,36)} = 0.1584$, $P = 0.6930$), no effect of AAV construct ($F_{(1, 36)} = 1.685$, $p = 0.2025$) but an effect of hemisphere ($F_{(1, 36)} = 27.60$, $P < 0.0001$). In the striatum however, the two way ANOVA revealed AAV construct × hemisphere interaction ($F_{(1,36)} = 45.85$, $P < 0.0001$), an effect of AAV construct ($F_{(1, 36)} = 29.85$, $P < 0.0001$) and an

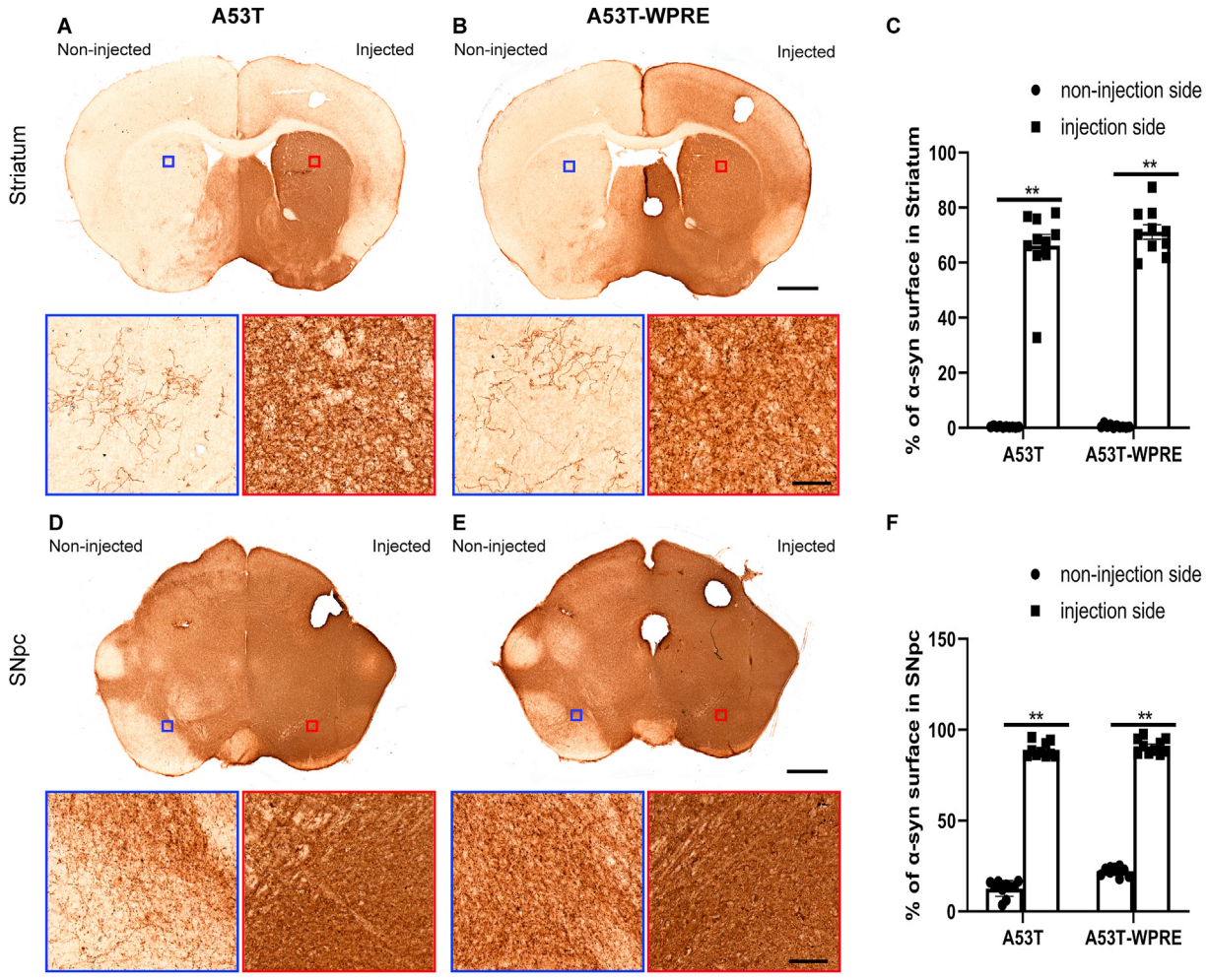

Figure 1. α-Synuclein expression at striatal (A–C) and mesencephalic (D–F) levels 12 weeks after intranigral injection of AAV2/9-synapsin-synA53T (A,D) and AAV2/9-synapsin-synA53T-WPRE (B,E). Representative images (Scale bars: 1.0 mm for striatum, 0.5 mm for SNpc) and surface quantification of hα-syn immunostaining in striatum (A–C) and SNpc (D–F) are displayed. Higher magnification pictures are shown (Scale bar: 40 μm) below each representative image. Data are expressed as mean percentage ±SEM of n = 10 mice per group. **p < 0.0001, compared to non-injected side.

effect of hemisphere ($F_{(1, 36)} = 249.5$, $P < 0.0001$). While both vectors significantly decreased the number of tyrosine hydroxylase (TH)-immunopositive neurons in the ipsilateral SNpc (Figure 2 A-C), there was no difference between the two vectors for the achieved nigral degeneration ($p = 0.6312$). However, AAV2/9-synapsin-synA53T-WPRE achieved a significantly greater loss of TH-immunopositive fibers into the striatum (Figure 2 D-F), translating into a functional meaning the apparent further decrease in the number of TH-immunopositive neurons (33% vs. 27% for AAV2/9-synapsin-synA53T, Figure 2 C).

3.3. AAV2/9-synapsin-synA53T -WPRE induced greater synucleinopathy

In the SNpc, there was no AAV construct × hemisphere interaction ($F_{(1,36)} = 1.313$, $P = 0.2595$), no effect of AAV construct ($F_{(1, 36)} = 1.211$, $p = 0.2785$) but an effect of hemisphere ($F_{(1, 36)} = 321.8$, $P < 0.0001$) for the level of S129 phosphorylated α-syn (pS129 α-syn). In the striatum however, there was an AAV construct × hemisphere interaction ($F_{(1,36)} = 10.63$, $P = 0.0024$), an effect of AAV construct ($F_{(1, 36)} = 10.45$, $p = 0.0026$) and an effect of hemisphere ($F_{(1, 36)} = 59.35$, $P < 0.0001$). Both vectors induced a strong significant punctiform pS129 α-syn immunoreactivity in both the striatum and the SNpc (Figure 3) leading to significant increase compared to the non-injected hemisphere. AAV2/9-synapsin-synA53T-WPRE achieved however a significantly greater punctiform pS129 α-syn immunoreactivity (Figure 3) in the striatum (Figure 3 A-C) compared to AAV2/9-synapsin-synA53T. While cortical staining represents a diffuse staining through the parenchyma, the striatal staining is highly punctiform and describes also Lewy neurites-like structures (insets of Figure 3A-B).

3.4. AAV2/9-synapsin-synA53T-WPRE elicited forelimb use asymmetry

An extent of nigral loss of 50% is classically required to observe overt parkinsonian motor symptoms (Bezard et al., 2001; Fearnley and Lees, 1991; Kordower et al., 2013), a threshold that was not reached in any of the groups. Nevertheless, subtle motor abnormalities can be detected below that threshold. There was no difference in the total number of steps (Figure 4A), errors per step (Figure 4B) and total time to traverse the beam (Figure 4C) in the challenging beam test between AAV2/9-synapsin-synA53T and AAV2/9- synapsin-synA53T-WPRE groups. In the cylinder test, there was no interaction effect on mice contacts (% of total contacts) between AAV construct and hemisphere ($F_{(1,36)} = 1.080$, $P = 0.305$) and no effect of AAV construct ($F_{(1, 36)} = 0.055$, $p = 0.814$), but there was a main effect of hemisphere ($F_{(1, 36)} = 6.587$, $P = 0.014$) suggestive of a differential impairment between the groups. AAV2/9-synapsin-synA53T-WPRE mice, but not AAV2/9-synapsin-synA53T mice, displayed a trend to a forelimb use

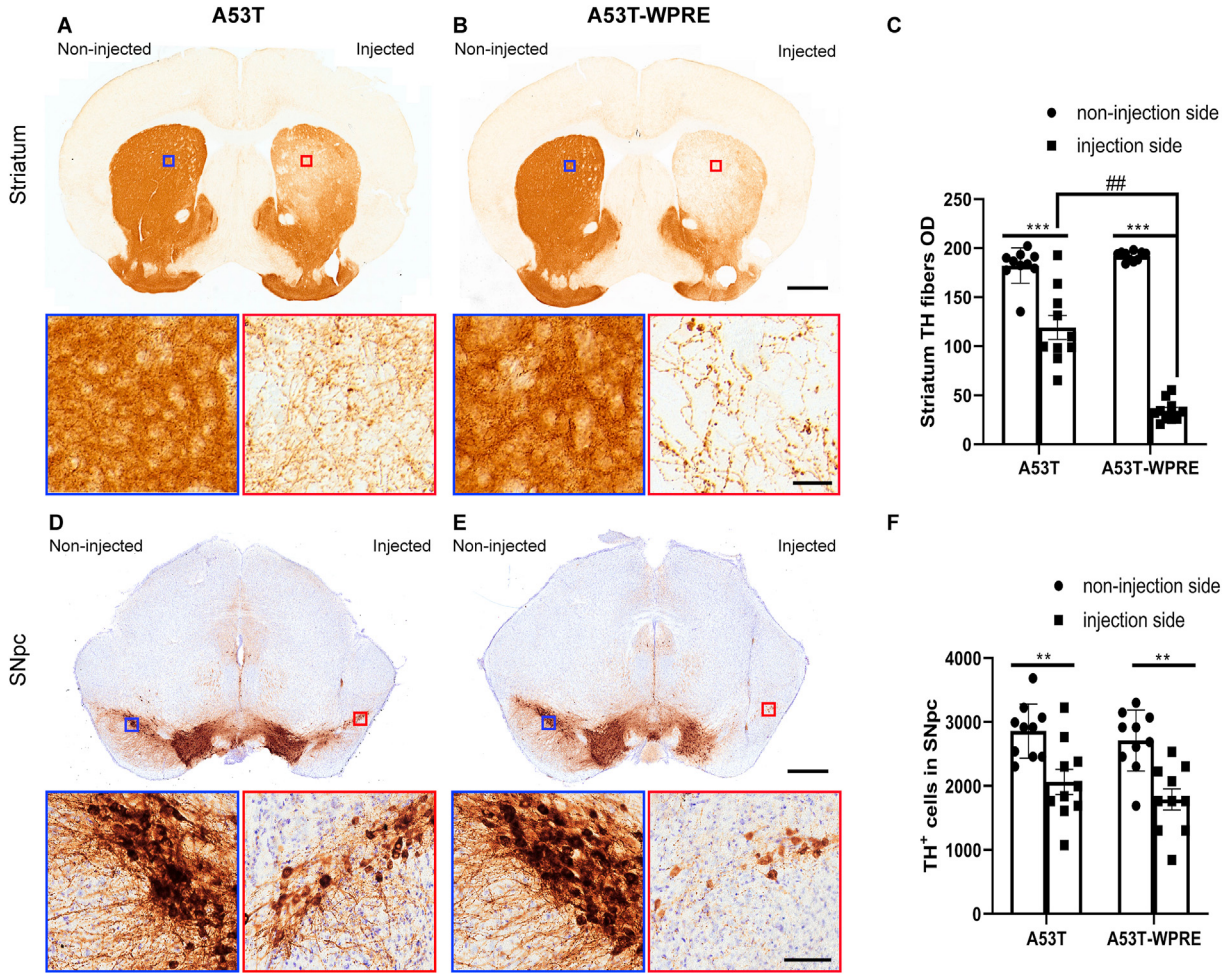

Figure 2. TH expression at striatal (A–C) and mesencephalic (D–F) levels 12 weeks after intranigral injection of AAV2/9-synapsin-synA53T (A,D) and AAV2/9-synapsin-synA53T-WPRE (B,E). AAV2/9-synapsin-synA53T and AAV2/9-synapsin-synA53T-WPRE induced degeneration of dopaminergic neurons as assessed by analysis of optical density of striatal TH-positive terminals (representative images: A, B; quantification: C) and by stereological quantification of TH-positive cells in SNpc (representative images:D, E; quantification: F). Scale bar: 0.5 mm for SNpc and 1 mm for striatum. Higher magnification pictures are shown (Scale bar: 100 μm for straitum and 40 μm for SNpc) below each representative image. Data are expressed as mean ± SEM of 10 mice per group. **$p < 0.01$, ***$p < 0.0001$ compared to non-injected side. ##$p < 0.0001$, compared to AAV2/9-synapsin-synA53T.

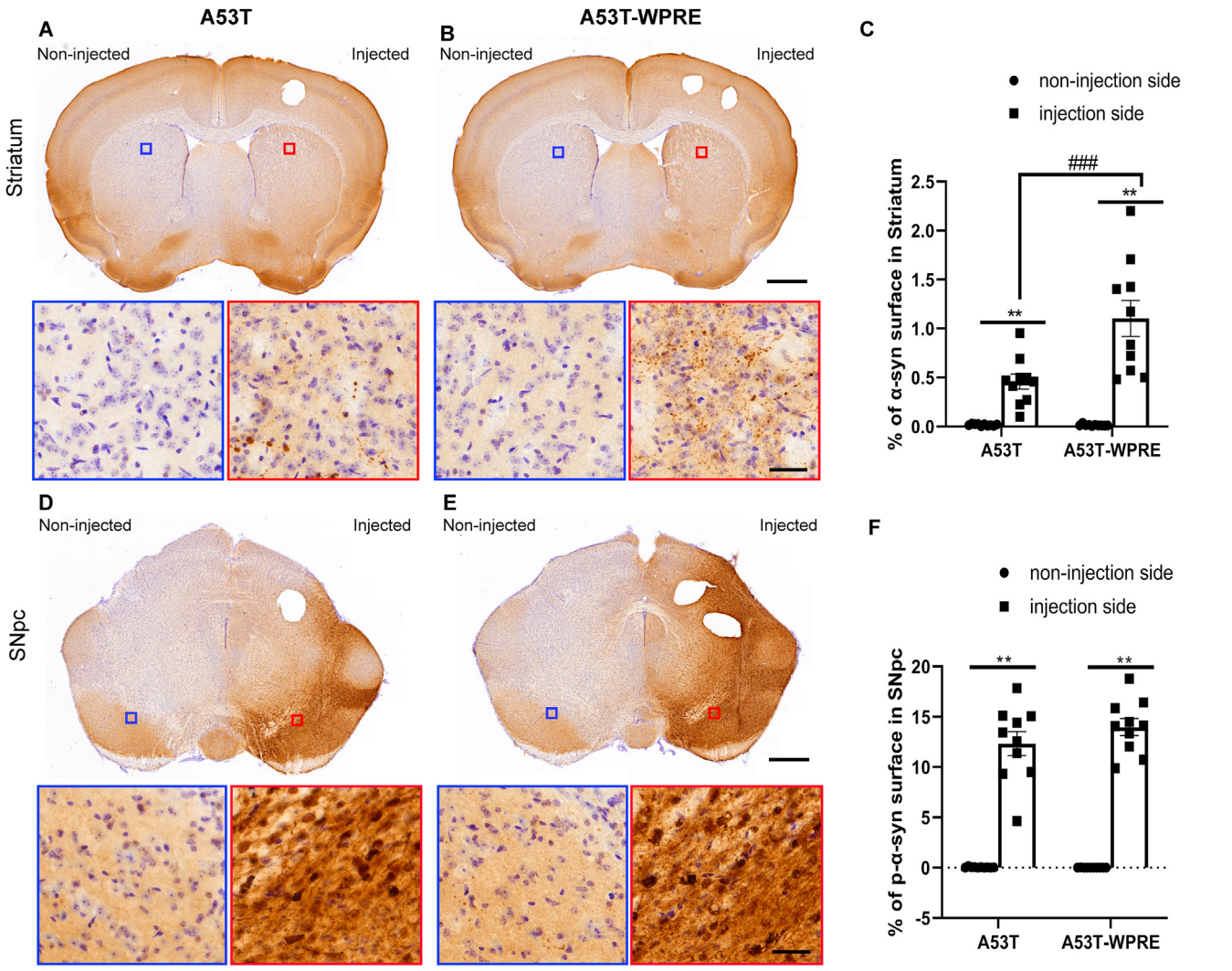

Figure 3. Immunodetection of α-synuclein phosphorylated at serine 129 (pS129) at striatal (A–C) and mesencephalic (D–F) levels 12 weeks after intranigral injection of AAV2/9-synapsin-synA53T (A,D) and AAV2/9-synapsin-synA53T-WPRE (B,E). AAV2/9-synapsin-synA53T and AAV2/9-synapsin-synA53T-WPRE induced increase in pS129 in striatum (representative images: A,B; quantification: C) and SNpc (representative images: D,E; quantification: F) Scales: 1.0 mm for Striatum, 0.5 mm for SNpc. Higher magnification pictures are shown (Scale bar: 40 μm) below each representative image). Data are expressed as mean percentage ±SEM of n = 10 mice per group. **p < 0.001 compared to non-injected side. ###p < 0.001, compared to AAV2/9-synapsin-synA53T.

asymmetry with preference for the ipsilateral (injection) side (Figure 4 D). No differences were found in asymmetry index (Figure 4E) and number of rearings (Figure 4F) between the AAV2/9-synapsin-synA53T and AAV2/9-synapsin-synA53T-WPRE mice.

4. Discussion

We here demonstrate that adding a WPRE to a classic AAV2/9-synapsin-synA53T construct achieves greater nigrostriatal degeneration (Figure 2) associated with nigral and striatal pS129 α-syn immunostaining (Figure 3), two anatomo-pathological landmarks that support the observed forelimb use asymmetry (Figure 4).

It has been shown that the magnitude of α-syn overexpression is a primary factor that determines the severity of dopaminergic neurons degeneration and subsequent motor deficits. Our study showed that both AAV2/9-synapsin-synA53T and AAV2/9-synapsin-synA53T-WPRE induced extensive expression of α-syn protein in both SNpc and striatum, in agreement with previous studies (Kirik et al., 2002). Overexpression of α-syn in the ipsilateral striatum indicated that A53T-hα-syn is transported along axons from neurons of SNpc to their fibers into the striatum. AAV2/9 and WPRE construct showed an improved tropism and spread of transgene product. Dopaminergic neurons loss in the SNpc is the most relevant neuropathological hallmark of PD, which determined the subsequent motor deficits.

In the present study, the hα-syn staining is not restricted to one hemisphere at the level of the SNpc (Figure 1D-F) but is mostly limited to it at the level of the striatum (Figure 1A-C)). One may question if this represents a (i) cell-to-cell spread of α-syn, (ii) a diffusion of α-syn throughout the matrix, (iii) an enormous spherical area of viral uptake and infection, or (iv) transfection of the interhemispheric dopaminergic projections. Diffusion of the protein at the mesencephalon rostro-caudal level seems involved in such bilateral staining as the whole ipsilateral hemisphere is also positively stained while only nigral cell bodies exhibit clear labelling compatible with true cellular expression of the transgene. Would cell-to-cell spread of α-syn be responsible then the very same bilateral staining would be present at the striatal level, which it is not. Volume of injection has been tailored so that the volume occupied by the injected solution remains limited to the SN, a volume checked prior actual experiments by dye injection checking. The very modest contralateral staining in the striatum is restricted to fibers (Figure 1A-B), an observation compatible with the tiny amount of interhemispheric dopamine neuron projections.

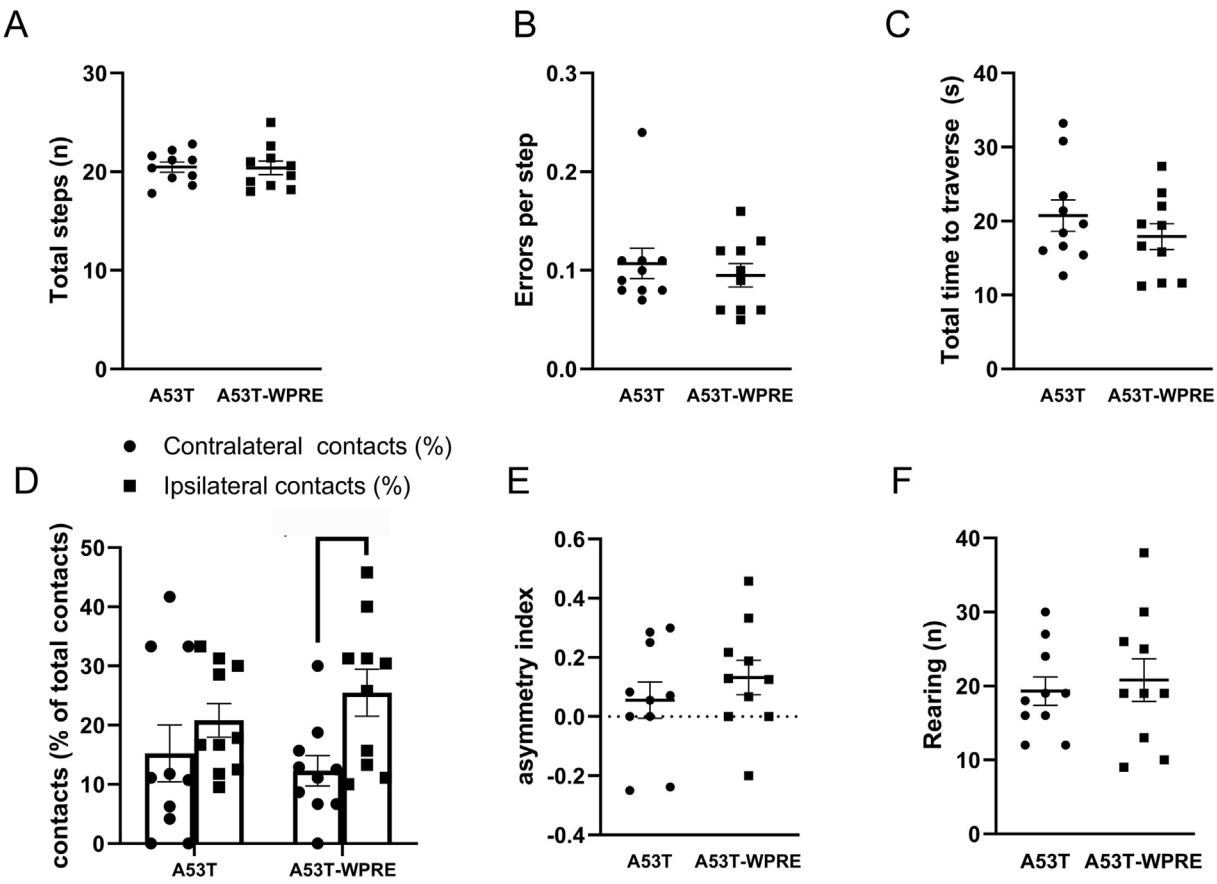

Figure 4. Effect of AAV2/9-synapsin-synA53T and AAV2/9-synapsin-synA53T-WPRE on the challenging beam test (A–C) and forelimb asymmetry in the cylinder test (D–F) assessed 12 weeks after injection. Data are expressed as mean ± SEM of 10 mice per group. D) Difference between both sides in AAV2/9-synapsin-synA53T-WPRE animals achieved p = 0.0691.

We observed that AAV2/9-synapsin-synA53T and AAV2/9-synapsin-synA53T-WPRE presented a 27% and 33% TH positive neurons reduction in the SNpc, respectively, in total agreement with previous studies showing that unilateral delivery of AAV-hα-syn induced about 30% dopaminergic neurons loss in SNpc in mice (Ip et al., 2017; Van der Perren et al., 2015). We have previously reported that mice presented a 30% SNpc dopamine neuron loss at 20 weeks after AAV2/9-mediated mutated human A53T α-syn. AAV2/9-synapsin-synA53T had a 35% optical density decrease of TH positive fibers in the striatum which is consistent with previous studies showing that the reduction of striatal TH positive fibers ranged from 20% at 9 weeks to 45% at 12 weeks (Ip et al., 2017; Song et al., 2015). However, AAV2/9- synapsin-synA53T-WPRE mice had an ipsilateral 82% loss of TH staining density of striatal fibers compared to the contralateral side and showed a 71% loss of TH signal compared to AAV2/9-synapsin-synA53T mice. Previous neuron tracing studies indicate that DA neurons from the dorsal tier of SNpc project to the matrix compartment of dorsal striatum, while neurons from the ventral tier send their axons to the complementary striosome or patch compartment (Sgobio et al., 2017). These circuits of mesencephalic dopaminergic neurons might explain the profound loss of TH in that part of the caudate-putamen achieved by WPRE presence and the observed behavioural asymmetry.

Generally, behavioural manifestation requires at least 50–60% loss of nigral dopaminergic neurons and striatal DA or TH fibers in rats and mice (Gombash et al., 2013; Kirik et al., 2002; Van der Perren et al., 2015). Unilateral delivery of AAV-hα-syn induces 20–30% dopaminergic neurons loss in mice, which often hinders the behavior deficits (Chesselet, 2008). We previously reported that bilateral AAV2/9 injection caused a 50% reduction of nigral DA neurons, which was accompanied by significant behavior deficits (Novello et al., 2018). In the current study, AAV2/9-synapsin-synA53T mice did not show the forelimb asymmetry, which is coherent with the level of about 30% dopaminergic neurons loss in the SNpc and striatum. AAV2/9-synapsin-synA53T-WPRE mice showed a slightly forelimb use asymmetry with preference for the ipsilateral side, which may be associated with an ipsilateral 82% loss of TH positive dopaminergic fiber terminals in striatum.

Phosphorylation at Ser-129 (pS129) of α-syn is an important pathological modification in synucleinopathy lesions (Anderson et al., 2006; Fujiwara et al., 2002) often taken as a proxy of aggregation. We observed that both AAV2/9-synapsin-synA53T and AAV 2/9-synapsin-synA53T-WPRE induced an extensive increase in pS129 α-syn immunostaining in the SNpc and striatum. In particular, AAV2/9-synapsin-synA53T-WPRE increased pS129 α-syn immunoreactivity significantly compared to AAV2/9-synapsin-synA53T. pS129 α-synuclein immunoreactivity and loss of TH positive striatal fiber terminals negatively correlated ($R^2 = 0.51$, $F_{(1,23)} = 24.4$, $p < 0.0001$) suggesting a causal relationship between dopaminergic denervation and a rise in pS129.

Our results are in agreement with previous work performed in rats and showing that the inclusion of a WPRE in the vector was required to obtain motor deficits and resulted in enhanced α-synuclein pathology and nigrostriatal degeneration (Decressac et al., 2012). Of note, both pathology and behavioral deficits in mice models of PD are commonly much less severe compared to the rat model. Rats indeed present larger lesions when challenged with neurotoxins and AAV-hα-syn, with up to 80% loss of SNpc dopaminergic neurons achieved by unilateral delivery of AAV-hα-syn (Bourdenx et al., 2015; Decressac et al., 2012). In another study, AAV6-synapsin-α-syn-WPRE treated rats displayed >70% loss of

SNpc TH positive cells and behavioral impairments 8 weeks after injection (Decressac et al., 2012). In non-human primates, we previously showed that A53T mutant α-syn over-expression induced 20 % dopamine neuron loss in aged marmoset monkeys after 11 weeks (Bourdenx et al., 2015). rAAV2/2 WT or A53T a-synuclein reportedly induced 30–40 % of the nigral cells loss that resulted in very mild motor deficits (Kirik et al., 2003; Koprich et al., 2016). The reason for the discrepancy of vulnerability to synuclein over-expression in different species remains unclear but certainly contains valuable information regarding the mechanisms underlying the resilience of some neurons to neurodegeneration.

5. Conclusion

In summary, we show that AAV2/9-synapsin-synA53T-WPRE achieved greater nigrostriatal degeneration and synucleinopathy which was concomitant with forelimb use asymmetry. This work helps refining a mouse PD model to be further used for unravelling molecular mechanisms of PD and screening novel potential therapies.

Declarations

Author contribution statement

Xiuping Sun, Xuan Yu, Ling Zhang, Wenjie Zhao, Manshi Wang, Yu Zhang, Xianglei Li, Sandra Dovero, Gregory Porras: Performed the experiments; Analyzed and interpreted the data; Wrote the paper.

Ran Gao: Performed the experiments; Wrote the paper.

Ludivine S. Breger, Pierre-Olivier Fernagut, Chuan Qin, Erwan Bezard: Conceived and designed the experiments; Wrote the paper.

Benjamin Dehay: Conceived and designed the experiments; Performed the experiments; Analyzed and interpreted the data; Wrote the paper.

Funding statement

This work was supported by National Natural Science Foundation of China Grant (31970510, 81941012), CAMS Innovation Fund for Medical Sciences (CIFMS) grant (2016-I2M-2-006, 2016-I2M-1-010) and SAFEA: Introduction of Overseas Talents in Cultural and Educational Sector (G20190001626).

Data availability statement

Data will be made available on request.

Declaration of interests statement

The authors declare no conflict of interest.

Additional information

No additional information is available for this paper.

Acknowledgements

We thank Dr. Nathalie Dutheil for AAV production.

References

Anderson, J.P., Walker, D.E., Goldstein, J.M., de Laat, R., Banducci, K., Caccavello, R.J., Barbour, R., Huang, J., Kling, K., Lee, M., et al., 2006. Phosphorylation of Ser-129 is the dominant pathological modification of alpha-synuclein in familial and sporadic Lewy body disease. J. Biol. Chem. 281, 29739–29752.

Arotcarena, M.L., Bourdenx, M., Dutheil, N., Thiolat, M.L., Doudnikoff, E., Dovero, S., Ballabio, A., Fernagut, P.O., Meissner, W.G., Bezard, E., et al., 2019. Transcription factor EB overexpression prevents neurodegeneration in experimental synucleinopathies. JCI insight 4.

Bezard, E., Dovero, S., Prunier, C., Ravenscroft, P., Chalon, S., Guilloteau, D., Crossman, A.R., Bioulac, B., Brotchie, J.M., Gross, C.E., 2001. Relationship between the appearance of symptoms and the level of nigrostriatal degeneration in a progressive 1-methyl-4-phenyl-1,2,3,6-tetrahydropyridine-lesioned macaque model of Parkinson's disease. J. Neurosci. 21, 6853–6861.

Bido, S., Soria, F.N., Fan, R.Z., Bezard, E., Tieu, K., 2017. Mitochondrial division inhibitor-1 is neuroprotective in the A53T-α-synuclein rat model of Parkinson's disease. Sci. Rep. 7, 7495.

Bourdenx, M., Dovero, S., Engeln, M., Bido, S., Bastide, M.F., Dutheil, N., Vollenweider, I., Baud, L., Piron, C., Grouthier, V., et al., 2015. Lack of additive role of ageing in nigrostriatal neurodegeneration triggered by α-synuclein overexpression. Acta Neuropath. Commun. 3, 46.

Chesselet, M.F., 2008. In vivo alpha-synuclein overexpression in rodents: a useful model of Parkinson's disease? Exp. Neurol. 209, 22–27.

Decressac, M., Mattsson, B., Lundblad, M., Weikop, P., Björklund, A., 2012. Progressive neurodegenerative and behavioural changes induced by AAV-mediated overexpression of α-synuclein in midbrain dopamine neurons. Neurobiol. Dis. 45, 939–953.

Dehay, B., Bourdenx, M., Gorry, P., Przedborski, S., Vila, M., Hunot, S., Singleton, A., Olanow, C.W., Merchant, K.M., Bezard, E., et al., 2015. Targeting alpha-synuclein for treatment of Parkinson's disease: mechanistic and therapeutic considerations. Lancet Neurol. 14, 855–866.

Engeln, M., Ansquer, S., Dugast, E., Bezard, E., Belin, D., Fernagut, P.O., 2016. Multifacetted impulsivity following nigral degeneration and dopamine replacement therapy. Neuropharmacology 109, 69–77.

Engeln, M., Fasano, S., Ahmed, S.H., Cador, M., Baekelandt, V., Bezard, E., Fernagut, P.O., 2013. Levodopa gains psychostimulant-like properties after nigral dopaminergic loss. Ann. Neurol. 74, 140–144.

Fearnley, J.M., Lees, A.J., 1991. Ageing and Parkinson's disease: substantia nigra regional selectivity. Brain 114 (Pt 5), 2283–2301.

Fleming, S.M., Ekhator, O.R., Ghisays, V., 2013. Assessment of sensorimotor function in mouse models of Parkinson's disease. JoVE.

Fujiwara, H., Hasegawa, M., Dohmae, N., Kawashima, A., Masliah, E., Goldberg, M.S., Shen, J., Takio, K., Iwatsubo, T., 2002. alpha-Synuclein is phosphorylated in synucleinopathy lesions. Nat. Cell Biol. 4, 160–164.

Gombash, S.E., Manfredsson, F.P., Kemp, C.J., Kuhn, N.C., Fleming, S.M., Egan, A.E., Grant, L.M., Ciucci, M.R., MacKeigan, J.P., Sortwell, C.E., 2013. Morphological and behavioral impact of AAV2/5-mediated overexpression of human wildtype alpha-synuclein in the rat nigrostriatal system. PloS One 8, e81426.

Hollensen, A.K., Thomsen, R., Bak, R.O., Petersen, C.C., Ermegaard, E.R., Aagaard, L., Damgaard, C.K., Mikkelsen, J.G., 2017. Improved microRNA Suppression by WPRE-Linked Tough Decoy microRNA Sponges, 23. RNA, New York, NY), pp. 1247–1258.

Ip, C.W., Klaus, L.C., Karikari, A.A., Visanji, N.P., Brotchie, J.M., Lang, A.E., Volkmann, J., Koprich, J.B., 2017. AAV1/2-induced overexpression of A53T-α-synuclein in the substantia nigra results in degeneration of the nigrostriatal system with Lewy-like pathology and motor impairment: a new mouse model for Parkinson's disease. Acta Neuropath. Commun. 5, 11.

Kalia, L.V., Lang, A.E., 2015. Parkinson's disease. Lancet 386, 896–912.

Kirik, D., Annett, L.E., Burger, C., Muzyczka, N., Mandel, R.J., Björklund, A., 2003. Nigrostriatal alpha-synucleinopathy induced by viral vector-mediated overexpression of human alpha-synuclein: a new primate model of Parkinson's disease. Proc. Natl. Acad. Sci. U. S. A. 100, 2884–2889.

Kirik, D., Rosenblad, C., Burger, C., Lundberg, C., Johansen, T.E., Muzyczka, N., Mandel, R.J., Björklund, A., 2002. Parkinson-like neurodegeneration induced by targeted overexpression of alpha-synuclein in the nigrostriatal system. J. Neurosci. 22, 2780–2791.

Klein, R., Ruttkowski, B., Knapp, E., Salmons, B., Gunzburg, W.H., Hohenadl, C., 2006. WPRE-mediated enhancement of gene expression is promoter and cell line specific. Gene 372, 153–161.

Koprich, J.B., Johnston, T.H., Reyes, G., Omana, V., Brotchie, J.M., 2016. Towards a non-human primate model of alpha-synucleinopathy for development of therapeutics for Parkinson's disease: optimization of AAV1/2 delivery parameters to drive sustained expression of alpha synuclein and dopaminergic degeneration in macaque. PloS One 11, e0167235.

Koprich, J.B., Johnston, T.H., Reyes, M.G., Sun, X., Brotchie, J.M., 2010. Expression of human A53T alpha-synuclein in the rat substantia nigra using a novel AAV1/2 vector produces a rapidly evolving pathology with protein aggregation, dystrophic neurite architecture and nigrostriatal degeneration with potential to model the pathology of Parkinson's disease. Mol. Neurodegener. 5, 43.

Kordower, J.H., Olanow, C.W., Dodiya, H.B., Chu, Y., Beach, T.G., Adler, C.H., Halliday, G.M., Bartus, R.T., 2013. Disease duration and the integrity of the nigrostriatal system in Parkinson's disease. Brain 136, 2419–2431.

Lo Bianco, C., Ridet, J.L., Schneider, B.L., Deglon, N., Aebischer, P., 2002. Alpha -Synucleinopathy and selective dopaminergic neuron loss in a rat lentiviral-based model of Parkinson's disease. Proc. Natl. Acad. Sci. U. S. A. 99, 10813–10818.

McFarland, N.R., Lee, J.S., Hyman, B.T., McLean, P.J., 2009. Comparison of transduction efficiency of recombinant AAV serotypes 1, 2, 5, and 8 in the rat nigrostriatal system. J. Neurochem. 109, 838–845.

Novello, S., Arcuri, L., Dovero, S., Dutheil, N., Shimshek, D.R., Bezard, E., Morari, M., 2018. G2019S LRRK2 mutation facilitates alpha-synuclein neuropathology in aged mice. Neurobiol. Dis. 120, 21–33.

Oliveras-Salvá, M., Van der Perren, A., Casadei, N., Stroobants, S., Nuber, S., D'Hooge, R., Van den Haute, C., Baekelandt, V., 2013. rAAV2/7 vector-mediated overexpression of alpha-synuclein in mouse substantia nigra induces protein aggregation and progressive dose-dependent neurodegeneration. Mol. Neurodegener. 8, 44.

Sgobio, C., Wu, J., Zheng, W., Chen, X., Pan, J., Salinas, A.G., Davis, M.I., Lovinger, D.M., Cai, H., 2017. Aldehyde dehydrogenase 1-positive nigrostriatal dopaminergic fibers exhibit distinct projection pattern and dopamine release dynamics at mouse dorsal striatum. Sci. Rep. 7, 5283.

Song, L.K., Ma, K.L., Yuan, Y.H., Mu, Z., Song, X.Y., Niu, F., Han, N., Chen, N.H., 2015. Targeted overexpression of alpha-synuclein by rAAV2/1 vectors induces progressive nigrostriatal degeneration and increases vulnerability to MPTP in mouse. PloS One 10, e0131281.

Soria, F.N., Engeln, M., Martinez-Vicente, M., Glangetas, C., López-González, M.J., Dovero, S., Dehay, B., Normand, E., Vila, M., Favereaux, A., et al., 2017. Glucocerebrosidase deficiency in dopaminergic neurons induces microglial activation without neurodegeneration. Hum. Mol. Genet. 26, 2603–2615.

St Martin, J.L., Klucken, J., Outeiro, T.F., Nguyen, P., Keller-McGandy, C., Cantuti-Castelvetri, I., Grammatopoulos, T.N., Standaert, D.G., Hyman, B.T., McLean, P.J., 2007. Dopaminergic neuron loss and up-regulation of chaperone protein mRNA induced by targeted over-expression of alpha-synuclein in mouse substantia nigra. J. Neurochem. 100, 1449–1457.

Van der Perren, A., Van den Haute, C., Baekelandt, V., 2015. Viral vector-based models of Parkinson's disease. Curr. Top Behav. Neurosci. 22, 271–301.

Zufferey, R., Donello, J.E., Trono, D., Hope, T.J., 1999. Woodchuck hepatitis virus posttranscriptional regulatory element enhances expression of transgenes delivered by retroviral vectors. J. Virol. 73, 2886–2892.